

# TrajMoE: Spatially-Aware Mixture of Experts for Unified Human Mobility Modeling

Chonghua Han, Yuan Yuan, Kaiyan Chen, Jingtao Ding, Yong Li  
Tsinghua University  
Beijing, China

## Abstract

Modeling human mobility across diverse cities is essential for applications such as urban planning, transportation optimization, and personalized services. However, generalization remains challenging due to heterogeneous spatial representations and mobility patterns across cities. Existing methods typically rely on numerical coordinates or require training city-specific models, limiting their scalability and transferability. We propose TrajMoE, a unified and scalable model for cross-city human mobility modeling. TrajMoE addresses two key challenges: (1) inconsistent spatial semantics across cities, and (2) diverse urban mobility patterns. To tackle these, we begin by designing a spatial semantic encoder that learns transferable location representations from POI-based functional semantics and visit patterns. Furthermore, we design a Spatially-Aware Mixture-of-Experts (SAMoE) Transformer that injects structured priors into experts specialized in distinct mobility semantics, along with a shared expert to capture city-invariant patterns and enable adaptive cross-city generalization. Extensive experiments demonstrate that TrajMoE achieves up to 27% relative improvement over competitive mobility foundation models after only one epoch of fine-tuning, and consistently outperforms full-data baselines using merely 5% of target city data. These results establish TrajMoE as a significant step toward realizing a truly generalizable, transferable, and pretrainable foundation model for human mobility.

## Keywords

Human mobility, Cross-city modeling, Mixture of experts

## 1 Introduction

Human mobility modeling plays a vital role in applications such as urban planning [25, 39, 40], transportation optimization [32, 33, 38], and personalized service [35, 37, 41]. With the rise of deep learning, recent work has begun exploring unified models to improve generalization and transferability in mobility-related tasks [10, 18, 21, 30, 44]. However, most existing approaches fall into one of three categories: (i) they operate within single-city settings, (ii) they use multi-city data but rely on semantically poor coordinate inputs, or (iii) they adopt separate encoders for each city to handle heterogeneous location spaces, limiting scalability and cross-city generalization.

Inspired by the success of pre-trained language models like GPT [1] and DeepSeek [9], we reformulate human mobility as sequences of semantically meaningful, discrete locations, enriched with spatial context such as POI distributions and visit frequency. This formulation aligns naturally with next-location prediction tasks and enables more expressive and transferable modeling of human movement. However, it also introduces two key challenges

for unified cross-city modeling. The first challenge concerns spatial representation. Unlike NLP, where tokens share a universal vocabulary, locations across cities are non-overlapping and lack inherent semantic correspondence. As a result, learning a unified representation space requires semantic alignment that goes beyond raw coordinate-based encoding. The second challenge lies in the heterogeneity of mobility patterns. Human movement behaviors differ significantly across cities due to variations in infrastructure, lifestyle, and geographic constraints. A unified model must be capable of capturing shared mobility principles while remaining adaptable to city-specific patterns.

To tackle these challenges, we propose **TrajMoE**, a unified and scalable model for cross-city human mobility modeling. At its core, TrajMoE is built on two key designs to support unified mobility representation learning. First, we design a spatial semantic encoder that constructs unified location representations by leveraging spatial attributes such as POI distribution and visit popularity. These attributes encode functional semantics, enabling consistent location embeddings across cities and forming the basis for spatial alignment. Second, we introduce the Spatially-Aware Mixture-of-Experts (SAMoE) Transformer, which adaptively routes trajectory features through a mixture of experts. To promote specialization and enhance generalization, we explicitly inject structured prior knowledge into each expert, allowing it to focus on a distinct mobility-related semantic (e.g., POI distribution, location popularity, or geographic coordinates). Additionally, a shared expert is introduced to jointly model all semantics, acting as a global expert that facilitates cross-city knowledge transfer and complements the specialized experts. Together, the encoder and SAMoE ensure both the feasibility and effectiveness of unified cross-city modeling by aligning spatial inputs and enabling adaptive knowledge transfer.

In summary, our contribution can be summarized as follows:

- We are the first to systematically address the challenge of building truly unified and scalable mobility models.
- We introduce TrajMoE, a unified and scalable framework for cross-city human mobility modeling, which integrates spatial semantic encoding and a spatially-aware mixture-of-experts Transformer to support unified and scalable representation learning.
- Extensive experiments on diverse city datasets demonstrate that TrajMoE achieves **state-of-the-art performance**, with a 27% relative improvement over existing mobility foundation models. It also exhibits strong transferability, outperforming full-data baselines using only 5% of the task-specific data.

## 2 Related Work

### 2.1 Mobility Prediction Models

The mobility prediction model forecasts users’ next location by modeling their historical trajectories. Early approaches primarily

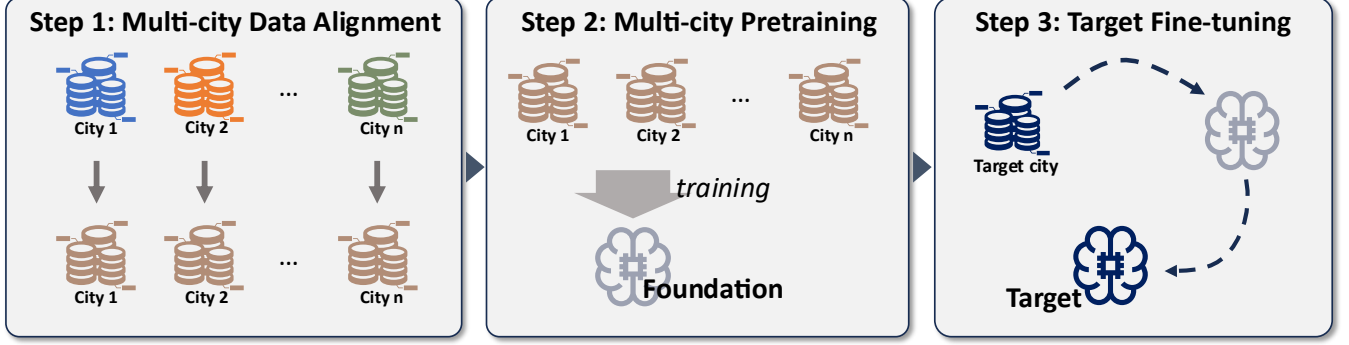


Figure 1: Illustration of the overall training process.

relied on probabilistic models, such as Markov models [3, 8] and EPR-based models [12, 24], which derived mobility patterns from transition probabilities between discrete locations. While effective in certain scenarios, these models often struggled to capture the complex dynamic characteristics of human behavior [7, 16], particularly when handling events with non-uniform and irregular time intervals. In recent years, deep learning models have significantly advanced mobility prediction. Techniques such as Recurrent Neural Networks (RNNs) [2, 36], attention networks [7, 34], Transformers [4, 23], Graph Neural Networks (GNNs) [26, 27], and diffusion models [20, 21, 43] have been widely applied to capture temporal dependencies in mobility data. However, separate models need to be trained for each city’s dataset. Several pre-trained mobility models [17, 44] have recently been proposed to enhance few-shot and zero-shot performance through large-scale foundational data pre-training. However, these models typically represent mobility behaviors as geographic coordinate movements. Consequently, they demonstrate limited capability in effectively modeling the intrinsic patterns of human mobility behavior.

## 2.2 Mixture of Experts

Mixture of Experts (MoE) [11, 13, 22] is a deep learning architecture that enhances model performance through a divide-and-conquer strategy. Its core idea lies in decomposing complex tasks and enabling collaborative processing by multiple specialized sub-models (experts), guided by a learnable gating network that dynamically allocates input data to the most relevant experts [42]. Each expert processes only a subset of inputs, significantly reducing computational costs, while the gating mechanism synthesizes final results through weighted aggregation of expert outputs [6, 15]. By maintaining the model’s parameter scale while improving inference efficiency, MoE has been widely adopted in large-scale language models [5, 15, 19], enabling trillion-parameter model deployment via sparse activation. However, challenges such as expert load balancing and training stability persist in its implementation.

## 3 Preliminaries

### 3.1 Human Mobility Data

Human mobility datasets record the movement trajectories of individuals across time and space with irregular time intervals and variable lengths. The relevant definitions are provided as follows:

**Definition of Location:** A location represents a discrete urban grid cell with unique identifier ID  $loc_i$ . The characteristics of each location include its geographic coordinates, Point of Interest (POI) distribution, and popularity. The latitude and longitude coordinates precisely pinpoint the area’s exact position in the city; the POI distribution reflects the functional attributes of the area; while popularity, measured by visit frequency over a given period, serves as a key indicator of its appeal and activity level.

**Definition of Mobility Trajectory:** A user’s mobility trajectory  $S_u$  is described as an irregular time series:

$$S_u = \langle loc_1, \tilde{t}_1 \rangle, \langle loc_2, \tilde{t}_2 \rangle, \dots, \langle loc_n, \tilde{t}_n \rangle \quad (1)$$

where  $\tilde{t}_i$  denotes the arrival time. Due to variations in individual mobility patterns, even when trajectory sequences share the same time window  $T$ , their sequence lengths  $n$  remain variable, with non-uniform time intervals between consecutive location points  $\tilde{t}_i$  and  $\tilde{t}_{i+1}$ .

### 3.2 Cross-City Mobility Prediction

The mobility prediction task requires estimating a user’s next location from variable-length history:

$$\widehat{loc}_{H+1} = \mathcal{F}(S_{1:H}), \quad S_{1:H} = \{\langle loc_1, \tilde{t}_1 \rangle, \dots, \langle loc_H, \tilde{t}_H \rangle\} \quad (2)$$

In the mobility prediction task, two critical distinctions merit attention: First, the phenomenon of geographic specificity leads to significant variations in location inventories across urban datasets  $\mathcal{D}_i$ , with spatial feature distributions exhibiting marked regional heterogeneity. Second, this geographic specificity directly results in model fragmentation within traditional approaches, necessitating city-specific model components for processing mobility sequences  $S_{1:H}$  in each urban subset  $\mathcal{D}_i \subseteq \mathcal{D}$ . More critically, when handling newly added urban data, existing methods require complete model retraining, severely constraining algorithmic scalability and practical applicability.

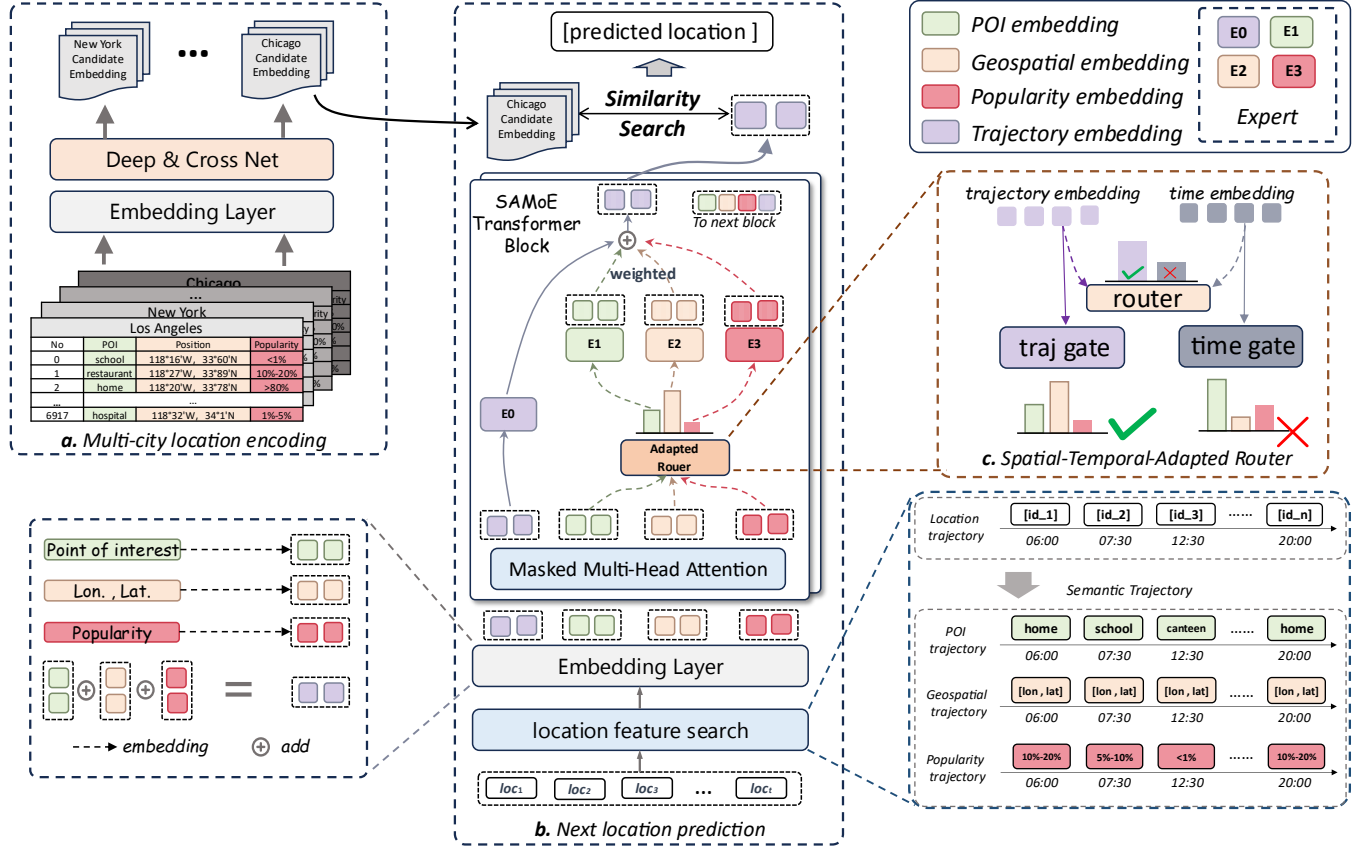


Figure 2: The overall architecture of TrajMoE. (a) Multi-city location encoding. (b) Next location prediction. (c) Spatial-temporal-adapted-router adaptively outputs the weights of the location spatial feature.

Our objective is to develop a universal prediction framework satisfying:

$$\widehat{loc}_{H+1} = \mathcal{F}(S_{1:H}), \quad \forall S \in \mathcal{D} = \bigcup_i \mathcal{D}_i \quad (3)$$

where the model maintains consistent architecture and parameterization across heterogeneous urban datasets. Additionally, when encountering new urban data  $\mathcal{D}_i \notin \mathcal{D}$ , the framework should require only minimal data fine-tuning to adapt to new urban mobility prediction tasks.

## 4 Methodology

### 4.1 Cross-city Location Encoding

We encode location candidates from different cities into spatial semantic embeddings using a unified encoder. When predicting the next location, for each user, the encoder only outputs the location embeddings of the city where the user's trajectory is located as the candidate database.

**4.1.1 Embedding Layer.** Each location is defined as a grid area, and the location embedding is obtained from three features: POI distribution  $\mathbf{P}$ , geographical coordinates  $\mathbf{G}$ , and popularity rank  $\mathbf{R}$ .

- POI distribution  $\mathbf{P} \in \mathbb{R}^{2c}$ , where  $c$  represents the number of POI categories and details are shown in Table 3. The POI distribution is encoded into the form  $[n_1, n_2, \dots, n_c, p_1, p_2, \dots, p_c]$ , where  $n_i$  denotes the number of POIs in the  $i$ -th category, and  $p_i = \frac{n_i}{\sum_{j=1}^c n_j}$ .
- Geographical coordinates  $\mathbf{G} \in \mathbb{R}^2$  refer to the latitude and longitude of the location's center point.
- $\mathbf{R} \in \mathbb{R}^1$  is a discrete integer value. Based on the flow data of all locations within the city, each location is ranked according to its popularity. The  $\mathbf{R}$  value is assigned based on the percentile ranking, which is shown in the Appendix Table 4.

We then create three embedding layers to obtain the following embeddings: POI embedding  $\mathbf{E}_p$ , geographical embedding  $\mathbf{E}_g$ , and flow rank embedding  $\mathbf{E}_r$ . The location embedding  $\mathbf{E}_l$  is defined as the sum of these three embeddings:

$$\mathbf{E}_l = \mathbf{E}_p + \mathbf{E}_g + \mathbf{E}_r. \quad (4)$$

**4.1.2 Deep & Cross Net.** Deep & Cross Net(DCN) [29] to further capture features from different locations. Figure 3 shows the architecture of DCN. Suppose that the input feature vector is location embedding  $\mathbf{E}_l$ , with a dimension of  $d$ . The Cross layer calculates as follows:

$$\mathbf{E}_{i+1} = \mathbf{E}_l \mathbf{E}_l^T \mathbf{W}_i + \mathbf{E}_i, \quad (5)$$

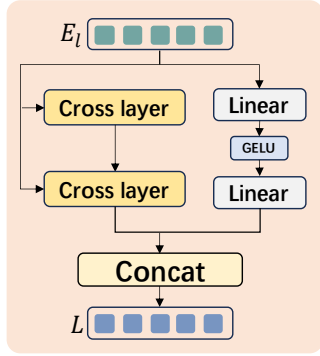


**Figure 3: The architecture of the Deep & Cross Net.**

where  $E_i$  represents the output of last cross layer, and  $W_i$  is the learnable weight matrix. The Deep layer further processes features through a multi-layer perceptron (MLP) structure. Its calculation method is as follows:

$$\mathbf{E}_{\text{deep}} = (\text{GELU}(\mathbf{W}_1 \mathbf{E}_1 + \mathbf{b}_1)) \mathbf{W}_2 + \mathbf{b}_2, \quad (6)$$

where  $\mathbf{W}_1$  and  $\mathbf{W}_2$  are learnable weight matrices,  $\mathbf{b}_1$  and  $\mathbf{b}_2$  are bias terms, and GELU is an activation function that introduces nonlinearity. The candidate locations embedding  $\mathbf{L} \in \mathbb{R}^{N \times d}$  is obtained by concatenating the outputs of the Cross layer and the Deep layer. The specific expression is as follows:

$$\mathbf{L} = \text{Concat}(\mathbf{E}_{\text{cross}}, \mathbf{E}_{\text{deep}}). \quad (7)$$

## 4.2 Spatially-Aware Mixture-of-Experts Transformer

Mobility trajectories exhibit significant heterogeneity across different cities. Directly mixing multi-city trajectory data for model training presents notable limitations: under a unified modeling framework, models either capture only cross-regional common mobility patterns while losing the ability to characterize city-specific features, or struggle to extract universal patterns due to divergent data distributions across cities. To address this, we design Spatially-Aware Mixture-of-Experts(SAMoE) Transformer, which integrates a shared Expert to capture universal behavioral patterns in mobility trajectories, while implementing personalized spatial representation enhancement on different locations across trajectories to effectively capture the unique characteristics of urban mobility patterns in different cities.

**4.2.1 Trajectory Embedding and Feature Merging.** The original trajectory  $S_u = \{loc_1, loc_2, \dots, loc_n\}$  is mapped into three new trajectories through the location feature search method illustrated in Figure 2:

$$S_f = \{x_1, x_2, \dots, x_n\}, \text{ where } x_i = (\text{POL}_i, \text{Position}_i, \text{Popularity}_i). \quad (8)$$

Each foundational trajectory is individually embedded to obtain  $E_{\text{poi}}$ ,  $E_{\text{pos}}$ , and  $E_{\text{pop}}$ . The fused trajectory embedding is initialized as:

$$E_{\text{traj}} = E_{\text{poi}} + E_{\text{pos}} + E_{\text{pop}}. \quad (9)$$

Additionally, temporal information of the trajectory is embedded into  $E_{ts}$ , defined as:

$$E_{ts} = \text{Emb}(tod) + \text{Emb}(dow) + \text{Emb}(\text{stay duration}), \quad (10)$$

where  $\text{Emb}(\cdot)$  denotes an embedding layer, *tod* is the **time of day**, and *dow* is the **day of week**.  $E_{ts}$  replaces the traditional positional encoding in Transformer architectures. It is combined with trajectory embeddings (e.g.,  $E_{\text{traj}}$ ) and serves as input to the attention layers

**4.2.2 Masked Multi-Head Attention.** The masked multi-head attention mechanism in our model incorporates two types of masks to ensure proper information flow and handle variable-length trajectories:

- **Causal Mask:** The causal mask ensures that the prediction at the  $i_{\text{th}}$  location is constrained to utilize information solely from the first  $i - 1$  locations. Specifically, it enforces a unidirectional dependency structure, where each location is influenced exclusively by its preceding locations. This design is essential for modeling sequential patterns in trajectories, as it effectively prevents the leakage of future information and preserves the temporal order inherent in the trajectory data.
- **Padding Mask:** Since the lengths of user's trajectories vary, we standardize the input length for the model by padding all trajectories to a fixed length of  $T$ . The padding mask ensures that the padded tokens do not affect the model's computational process. This padding strategy ensures that the model can process trajectories of different lengths while maintaining the integrity of the original data structure.

The attention layer processes the four trajectory embeddings  $E$  separately, and through residual connections and layer normalization, obtains the token representations  $H$  of the four trajectories as input to the SAMoE block.

$$H_{\text{POI}} = \text{Attention}(E_{\text{POI}} + E_{ts}), \quad (11)$$

$$H_{\text{pos}} = \text{Attention}(E_{\text{pos}} + E_{ts}), \quad (12)$$

$$H_{\text{pop}} = \text{Attention}(E_{\text{pop}} + E_{ts}), \quad (13)$$

$$H_{\text{traj}} = \text{Attention}(E_{\text{traj}} + E_{ts}). \quad (14)$$

**4.2.3 Spatial-Temporal-Adapted Router(STAR).** Our approach addresses the substantial spatiotemporal variations in urban mobility patterns by introducing a Spatial-Temporal-Adapted Router that dynamically selects foundational trajectory representations based on temporal information and historical mobility behaviors to enhance fused trajectory characterization. Specifically, the router employs three gating networks based on a linear layer:

- Traj-gate computes weights for three foundational trajectory representations using historical trajectory patterns;
- Time-gate that derives weighting schemes from temporal feature representations;
- Adapted router adaptively determines the final weighting strategy by jointly analyzing both historical trajectories and temporal contexts, thereby selects between the outputs of the traj-gate and time-gate to guide the MoE block’s expert weight.

STAR's operation can be formally expressed as:

$$\begin{aligned}
 w_{\text{traj}} &= \text{TrajGate}(H_{\text{traj}}), & (\text{Trajectory Weight}) \\
 w_{\text{time}} &= \text{TimeGate}(E_{\text{ts}}), & (\text{Temporal Weight}) \\
 [s_1, s_2] &= \text{AdaptedRouter}(H_{\text{traj}} \| E_{\text{ts}}), & (\text{Adaptation Scores}) \\
 g &= \begin{cases} 1, & \text{if } s_1 \geq s_2 \\ 0, & \text{otherwise} \end{cases} & (\text{Weight Selector}) \\
 W &= g \cdot w_{\text{traj}} + (1 - g) \cdot w_{\text{time}}, & (\text{Final Weight})
 \end{aligned}$$

The weight vector  $W \in \mathbb{R}^3$  represents the importance scores for three foundational trajectory embeddings.

**4.2.4 Spatially-Aware Mixture-of-Experts.** The human mobility trajectories exhibit shared intent-driven patterns across cities while maintaining structural heterogeneity. To better model urban mobility trajectories across cities, we employ a Spatially-Aware Mixture-of-Experts framework, which learns universal patterns of human mobility through a fused trajectory Expert. Simultaneously, a Spatial-Temporal-Adapted Router is utilized to selectively enhance the fused trajectory representations by adaptively weighting different foundational trajectory experts, thereby capturing the heterogeneity of trajectories across different cities. The computational formulation can be expressed as:

$$H'_i = \text{Expert}_i(H_i), \forall i \in \{\text{poi}, \text{pos}, \text{pop}\}, \quad (15)$$

$$W = \text{STAR}(\mathcal{H}_{\text{traj}}, E_{\text{ts}}), \quad (16)$$

$$H'_{\text{traj}} = \text{Expert}_0(H_{\text{traj}}) + \sum_{i=1}^3 w_i H'_i. \quad (17)$$

**4.2.5 Prediction Layer.** Given the final fused trajectory representation  $H_{\text{traj}}$ , we can finally predict the next potential location according to the following probability:

$$P(i_{t+1}|t) = \text{Softmax}(H_{\text{traj}} \cdot l_{i_{t+1}}), \quad (18)$$

where we calculate the softmax probability over the candidate location set, and  $l_{i_{t+1}}$  is the embedding representation of item  $i_{t+1}$  from the embedding matrix  $L$  (see Eq 7).

### 4.3 Cross-city Pretraining and Supervised Fine-Tuning

We propose a two-phase training paradigm for TrajMoE to achieve effective knowledge transfer across urban mobility patterns. The framework consists of Cross-City Pretraining and Target City Adaptation.

On the first phase, TrajMoE is pretrained on mobility trajectory datasets spanning multiple urban environments, enabling comprehensive learning of universal movement patterns and spatial-temporal dependencies across diverse city layouts. As detailed in Algorithm 1, during the training process, a batch of trajectory data is extracted from the dataset of a random city. The user's historical trajectory data is fed into the SAMoE Transformer to derive the intent embedding  $H_{\text{traj}}$  for the history trajectory representation. Concurrently, the features of all locations within the city are input into the DCN to generate the location candidates embedding  $L$ . The final **logits** is computed through element-wise multiplication of  $L$  and  $H_{\text{traj}}$  and the loss is expressed as:

$$\text{Loss} = \text{Cross-Entropy Loss}(\text{logits}, \text{loc}_{t+1}), \quad (19)$$

---

#### Algorithm 1 Unified Pretraining

---

**Require:** Trajectory dataset  $\mathcal{D} = \{\mathcal{D}_1, \mathcal{D}_2, \dots, \mathcal{D}_M\}$  from  $M$  cities, model with parameters  $\theta$ , Loss function  $\mathcal{L}_{\text{CE}}$  (Cross Entropy).

**Ensure:** Learnable parameters  $\theta$  for the model.

```

1: for  $epoch \in \{1, 2, \dots, N_{\text{iter}}\}$  do
2:   Randomly sample a mini-batch  $\mathcal{B}$  from a random city dataset  $\mathcal{D}_m$ .
3:   for each trajectory  $S = \{loc_1, t_1, loc_2, t_2, \dots, loc_n, t_n\} \in \mathcal{B}$  do
4:     Generate foundational trajectories and time sequence:
       POI trajectory  $P = \{POI_1, POI_2, \dots, POI_n\}$ ,
       Position trajectory  $G = \{pos_1, pos_2, \dots, pos_n\}$ 
       Popularity trajectory  $R = \{pop_1, pop_2, \dots, pop_n\}$ 
       Time sequence  $ts = \{t_1, t_2, \dots, t_n\}$ 
5:      $E_{\text{POI}}, E_{\text{pos}}, E_{\text{pop}} \leftarrow \text{emb}(P), \text{emb}(G), \text{emb}(R)$ 
6:      $E_{\text{traj}} = E_{\text{POI}} + E_{\text{pos}} + E_{\text{pop}}$ 
7:      $E_{\text{ts}} \leftarrow \text{emb}(ts)$ 
8:      $H'_{\text{traj}} = \text{SAMoE Transformer}(E_{\text{POI}}, E_{\text{pos}}, E_{\text{pop}}, E_{\text{traj}}, E_{\text{ts}})$ 
9:     Retrieve location candidates:  $N_{\text{loc}} = (P_l, G_l, R_l)$ 
10:     $E_P, E_G, E_R \leftarrow \text{emb}(P_l), \text{emb}(G_l), \text{emb}(R_l)$ 
11:     $\mathcal{L} = \text{DCN}(E_P + E_G + E_R)$ 
12:    Compute logits:  $\text{logits} = \text{Softmax}(H'_{\text{traj}} \odot \mathcal{L})$ .
13:    Calculate loss:  $\text{Loss} \leftarrow \mathcal{L}_{\text{CE}}(\text{logits}, \text{loc}_{t+1})$ .
14:  end for
15:  Update the model's parameters  $\theta \leftarrow \text{update}(\text{Loss}; \theta)$ 
16: end for

```

---

where  $\text{loc}_{t+1}$  is the true next location id.

After acquiring generic mobility patterns through pretraining, the model can efficiently adapt to target urban characteristics via single-epoch supervised fine-tuning, achieving an optimal balance between generalization capacity and location-aware personalization.

## 5 Results

### 5.1 Experiment Setting

**5.1.1 Dataset.** We conduct extensive experiments on six real-world mobility datasets: Atlanta, Chicago, Seattle, Washington, New York, Los Angeles. Detailed information on the data sets is summarized in Appendix Table 2. For pre-processing the trajectory data in these datasets, we applied a sliding window of three days to each user's trajectory and filtered out trajectories with fewer than five trajectory points. For every location, POI data is sourced from Open Street Map and consists of 34 major categories, and the details are shown in Table 3. The longitude and latitude of all locations in the same city are normalized to have a mean of 0 and a standard deviation of 1. We discrete the popularity rank based on quintiles, and details are shown in Tables 4. For temporal pre-processing, we divide a day into 48 time slots at half-hour intervals and map  $t_i$  to the nearest discrete time point.

**5.1.2 Metrics.** Evaluation metric  $\text{Acc@K}$  is utilized to measure the proportion of samples that are correctly predicted within the top  $K$  highest-probability locations by the model. The formula for  $\text{Acc@k}$

**Table 1: Performance comparison of different prediction models in terms of Acc@k, where bold denotes the best results, underline denotes the second best.**

City	Metric	Markov	LSTM	Transformer	DeepMove	TrajBert	GETNext	CTLE	TrajFM	Unitraj	TrajMoE (w/o pretrain)	TrajMoE	Improv.
Atlanta	Acc@1	0.183	0.231	0.210	0.242	0.213	0.233	0.263	0.265	0.283	<u>0.285</u>	<b>0.331</b>	17.0% ↑
	Acc@3	0.325	0.373	0.353	0.393	0.369	0.402	0.422	0.421	0.421	<u>0.423</u>	<b>0.467</b>	10.7% ↑
	Acc@5	0.388	0.458	0.444	0.467	0.453	0.476	<u>0.500</u>	0.492	0.490	0.488	<b>0.532</b>	6.4% ↑
Chicago	Acc@1	0.146	0.194	0.175	0.203	0.182	0.184	0.200	0.208	0.215	<u>0.235</u>	<b>0.277</b>	28.8% ↑
	Acc@3	0.260	0.334	0.300	<u>0.344</u>	0.316	0.324	0.341	0.341	0.342	0.330	<b>0.371</b>	7.8% ↑
	Acc@5	0.316	0.404	0.383	0.415	0.394	0.404	<u>0.417</u>	<u>0.417</u>	<u>0.417</u>	0.389	<b>0.418</b>	0.2% ↑
Seattle	Acc@1	0.202	0.259	0.235	0.277	0.234	0.255	0.289	0.311	<u>0.332</u>	0.321	<b>0.363</b>	9.3% ↑
	Acc@3	0.318	0.420	0.397	0.444	0.401	0.424	0.454	0.466	<u>0.478</u>	0.467	<b>0.509</b>	6.5% ↑
	Acc@5	0.423	0.507	0.494	0.524	0.494	0.508	0.536	0.549	<u>0.551</u>	0.536	<b>0.576</b>	4.5% ↑
Washington	Acc@1	0.162	0.224	0.192	0.246	0.207	0.225	0.232	0.243	0.259	<u>0.272</u>	<b>0.319</b>	23.2% ↑
	Acc@3	0.347	0.383	0.356	0.407	0.367	0.387	0.390	0.420	<u>0.423</u>	0.409	<b>0.452</b>	6.9% ↑
	Acc@5	0.419	0.463	0.450	0.486	0.457	0.470	0.474	0.476	<u>0.496</u>	0.477	<b>0.517</b>	4.2% ↑
New York	Acc@1	0.115	0.169	0.156	0.176	0.159	0.158	0.156	0.178	0.188	<u>0.205</u>	<b>0.264</b>	40.4% ↑
	Acc@3	0.275	0.312	0.318	0.328	0.310	0.310	0.313	0.333	<u>0.335</u>	0.329	<b>0.386</b>	15.2% ↑
	Acc@5	0.330	0.406	0.383	0.410	0.400	0.415	0.435	0.439	<u>0.442</u>	0.394	<b>0.446</b>	0.9% ↑
Los Angeles	Acc@1	0.103	0.131	0.124	0.146	0.146	0.139	0.138	0.142	0.166	<u>0.188</u>	<b>0.244</b>	47.0% ↑
	Acc@3	0.201	0.275	0.268	0.273	0.277	0.276	0.275	0.276	<u>0.277</u>	<u>0.289</u>	<b>0.341</b>	23.1% ↑
	Acc@5	0.315	0.349	0.337	0.344	0.352	0.352	0.354	0.360	<u>0.367</u>	0.341	<b>0.390</b>	6.3% ↑

can be expressed as follows:

$$\text{Acc}@k = \frac{1}{N} \sum_{i=1}^N \mathbb{I}(y_i \in \{f(x_i)_1, f(x_i)_2, \dots, f(x_i)_k\}) \quad (20)$$

where  $\mathbb{I}(\cdot)$  is the indicator function (1 if the condition is true, 0 otherwise),  $N$  is the total number of samples,  $y_i$  is the true label for the  $i$ -th sample,  $f(x_i)_1, \dots, f(x_i)_k$  are the top  $k$  predictions made by the model for the sample  $x_i$ .

**5.1.3 Baselines.** We compared our method with state-of-the-art models. These baselines collectively represent diverse technical directions for trajectory modeling.

- **Traditional statistical method:** The Markov model serves as a statistical framework designed to depict how states evolve over time. It predicts future locations by computing the probabilities of transitions.
- **Sequence modeling methods:** LSTM [14] networks excel at processing sequential data and are adept at capturing long-term dependencies, making them naturally suitable for location prediction tasks. Transformer [28]: Transformer is a deep learning architecture based on the self-attention mechanism, capable of efficiently processing sequential data and capturing long-range dependencies.
- **Deep mobility methods:** DeepMove [7] is a popular mobility prediction baseline. TrajBERT [23] is a trajectory recovery method based on BERT, which recovers implicit sparse trajectories through spatial-temporal refinement. GETNext [31] integrates Graph Convolutional Networks (GCN) and Transformer to model global POI transition patterns via a trajectory flow map. It fuses spatio-temporal contexts with time-aware category embeddings for next POI recommendation.
- **Pretrained trajectory foundation methods:** We incorporate CTLE [17], TrajFM [18] and UniTraj [44], which employ large-scale pretraining with strategies like trajectory masking-recovery

and multi-strategic resampling to achieve adaptive, context-aware embeddings and superior cross-domain transferability.

**5.1.4 Implementation Details.** We first pretrain TrajMoE on five cities and subsequently fine-tuned it for 1 epoch using data from the remaining city. The SAMoE transformer blocks utilized in this study comprise 4 layers, with an embedding dimension of 512. Pretraining was conducted using the AdamW optimizer, with a learning rate set to  $3 \times 10^{-4}$ , for a total of 50 epochs. Early stopping was implemented to terminate training if the validation loss did not improve for 3 consecutive epochs. The batch size was fixed at 16. We conducted a 6-hour pretraining using eight NVIDIA A800-SXM4-40GB GPUs.

## 5.2 Overall Performance

We conducted comprehensive comparative experiments between TrajMoE and baseline methods across six datasets. Due to the baseline models' inability to simultaneously handle datasets from multiple cities with varying numbers of locations, we trained each baseline exclusively on individual datasets. For TrajMoE, we present both single-dataset training results and the outcomes of our pre-training followed by fine-tuning approach. The comparative performance metrics for all experimental configurations are systematically presented in Table 1. Based on the experimental findings, we have reached the following conclusions:

- **TrajMoE outperforms the state-of-the-art baselines in the mobility prediction task.** On the Los Angeles and New York datasets, fine-tuning our pretrained TrajMoE achieves a remarkable 40% relative improvement in Acc@1 performance compared to the suboptimal SOTA baseline, with an absolute accuracy gain of 8%. Across all datasets, TrajMoE demonstrates consistent improvements in all metrics, with the most significant enhancement observed on Acc@1—achieving an average relative performance improvement of over 20%. Even in the worst-case scenario on the Seattle dataset, it still delivers a notable relative improvement of 9.3%.



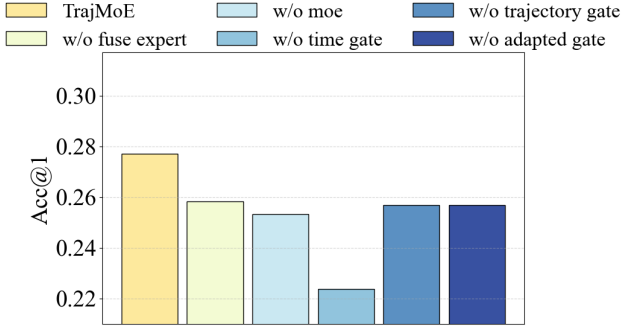


Figure 4: Ablation study on the SAMoE design using Acc@1 on Chicago dataset.

- **TrajMoE achieves state-of-the-art or near-SOTA performance when trained exclusively on single-city datasets.** Even without prior pre-training on other datasets, TrajMoE achieves state-of-the-art (SOTA) performance on the Acc@1 metric across most datasets, while Acc@3 and Acc@5 demonstrate SOTA or near-SOTA performance. This demonstrates its architectural superiority in effectively capturing urban-specific mobility patterns without relying on cross-domain knowledge transfer. This observation further confirms that the model’s design principles fundamentally enhance representation learning for trajectory modeling across different operational scales.

TrajMoE demonstrates superior performance, suggesting that training a universal mobility model across different cities holds huge potential for improving prediction accuracy and generalization capabilities. This demonstrates TrajMoE’s capability to capture underlying universal patterns of human mobility despite structural and socioeconomic disparities across cities, while effectively transferring this cross-city knowledge to new urban trajectory prediction tasks. The findings not only validate the existence of transferable mobility principles across heterogeneous urban environments, but also establish a methodological foundation for exploring scaling laws in the human mobility area through larger datasets and model parameters.

### 5.3 Ablation Studies

SAMoE is the key design of TrajMoE, specifically addressing cross-city data heterogeneity through its specialized gating mechanisms. We conducted systematic ablation studies on five critical configurations: removal of (1) the adapted gate, (2) the time gate, (3) the traj-gate, (4) the MOE framework while retaining only the fuse expert, and (5) the fuse expert. Experimental results on Chicago and New York datasets are shown in Figure 4, and additional results are provided in the Appendix Table 5. The results demonstrate consistent performance degradation across all ablated variants. This empirical evidence confirms that each component collectively contributes to effective spatio-temporal pattern modeling, establishing SAMoE’s architectural elements as essential design choices for urban mobility prediction.

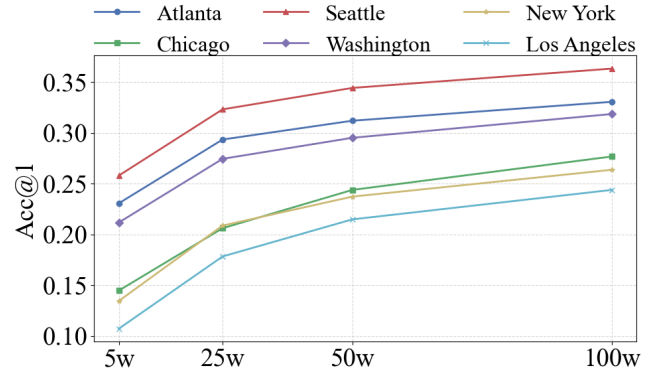


Figure 5: Performance evaluation (Acc@1) with varying volume of pre-train data.

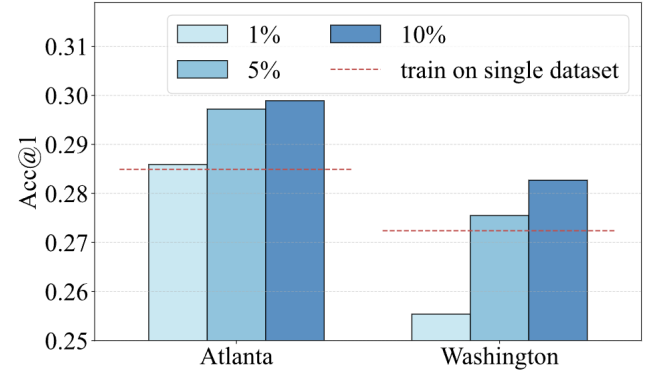


Figure 6: Cross-city Transfer Performance on Atlanta and Washington dataset.

### 5.4 Data Scalability

The superior performance of TrajMoE partially stems from its extensive pretraining on massive mobility data and subsequent knowledge transfer to target cities through fine-tuning. To validate the model’s data scaling capabilities, we conducted experiments using foundation models pretrained with varying data volumes and evaluated their fine-tuned performance. As shown in Figure 5 (with additional results in the Appendix C.2), we observe a consistent performance improvement in fine-tuned models as pretraining data increases, with no signs of performance plateauing observed. This compelling trend indicates that mobility foundation models hold significant potential for future development through continued data scaling, suggesting that current performance levels merely represent an intermediate stage rather than an upper bound.

### 5.5 Cross-city transfer performance

One significant advantage of employing large-scale data for model pretraining lies in the effective transfer of knowledge acquired from pretraining datasets to target cities. This enables the model to achieve superior prediction performance through minimal data fine-tuning in target domains. To systematically validate the model’s

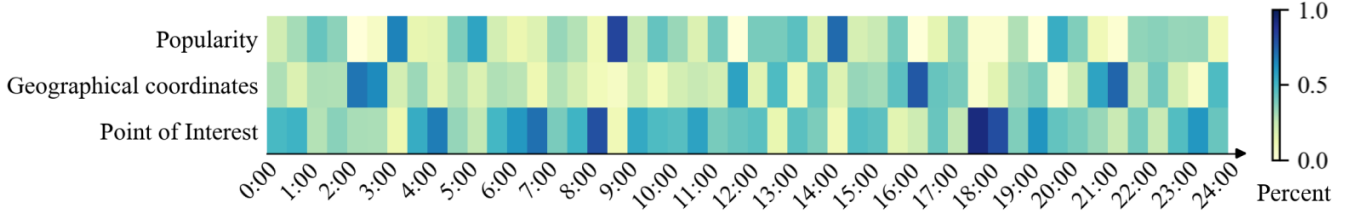


Figure 7: The top-1 percent of time gate during a day in TrajMoE.

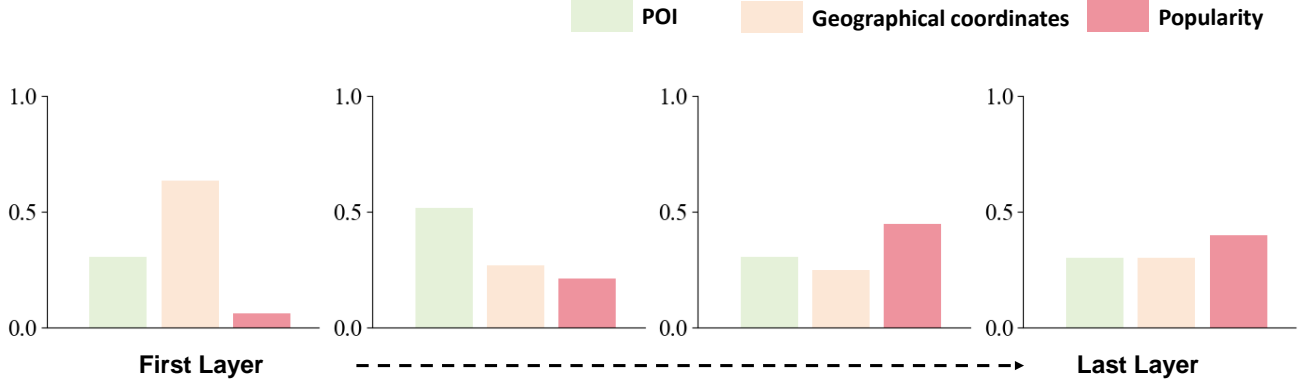


Figure 8: The distribution of trajectory gate weights across different layers in TrajMoE.

generalization capability, we conducted experiments with 1%, 5%, and 10% of target city data for single-epoch fine-tuning on the pre-trained model. As illustrated in Figure 6 (with additional results in the Appendix C.3), the results demonstrate that merely 5% of data for fine-tuning can match the performance achieved by training non-pretrained models with full datasets. This compelling evidence substantiates the exceptional generalization capacity of our pre-training methodology, highlighting its effectiveness in cross-city knowledge transfer with limited target data requirements.

### 5.6 Spatial-Time-Adapted Router analysis

As a key design of TrajMoE, we conduct comprehensive analyses of the statistical patterns exhibited by the Trajectory Gate and Time Gate within the Spatial-Time-Adapted Router framework, while visualizing how the model effectively captures the spatiotemporal characteristics of mobility trajectories during the training process.

- **Time Gate analysis:** Figure 7 presents our statistical analysis of Time gate’s percent of top1 weights across temporal dimensions. The results demonstrate the gate’s predominant focus on POI semantics throughout most temporal intervals, exhibiting remarkable consistency across different urban contexts. This indicates that compared to mere urban positional movements, human behavioral mobility with richer semantic representations—such as dining activities—better reflects the patterns of human movement.
- **Trajectory Gate analysis:** Figure 8 illustrates the output weight distributions of trajectory gates across different layers. Our analysis reveals distinct hierarchical learning patterns: initial layers

primarily capture fundamental geographical coordinate variations (latitude/longitude shifts), while deeper layers progressively model semantic patterns including Points of Interest (POI) interactions and location popularity dynamics. Notably, the final layer demonstrates balanced weight allocation across these three features, enabling their synergistic integration for the mobility prediction task.

## 6 Conclusion

In this paper, we present TrajMoE, a pre-trained foundation model designed for cross-city human mobility modeling through a spatially-aware mixture-of-experts architecture and unified semantic location encoding. By integrating semantically enriched location attributes and dynamically adapting to urban-specific mobility patterns, TrajMoE establishes a novel framework for capturing universal human movement dynamics while preserving city-specific characteristics. Extensive experiments demonstrate its superior performance and generalization capabilities in cross-city mobility prediction tasks, highlighting the effectiveness of our approach in bridging heterogeneous urban contexts.

We believe TrajMoE not only advances the understanding of transferable mobility principles but also sets a foundation for scalable spatio-temporal modeling across diverse urban ecosystems. Future research could explore extending this paradigm to larger-scale datasets and architectures, further harmonizing universal patterns with localized urban dynamics to empower intelligent urban systems and personalized mobility services.



## A Datasets

**Table 2: Basic statistics of mobility dataset.**

City	Duration	Location	Trajectory
Atlanta	7 days	1175	200000
Chicago	7 days	4166	200000
Seattle	7 days	1046	200000
Washington	7 days	1361	200000
New York	7 days	4988	200000
Los Angeles	7 days	6198	200000

## B Location Feature Details

The details of POI categories are shown in Table 3.

**Table 3: Details of POI Categories**

finance	café	dormitory	public
transport	ice cream	shop	livelihood
health	restaurant	travel agency	service
education	boutique	office	government
religion	retail	public transport	accommodation
food	marketplace	home improvement	tourism
fast food	residential	entertainment	pub
shop beauty	recycling	shop transport	kindergarten
commodity	sport		

The details of popularity rank and value are shown in Table 4.

**Table 4: Details of Popularity Rank and Value**

Popularity Rank	R value
<1%	0
1%-5%	1
5%-10%	2
10%-20%	3
20%-40%	4
40%-60%	5
60%-80%	6
>80%	7

## C Additional Results

### C.1 Ablation Study

Table 5 illustrates results of ablation study.

### C.2 Data Scalability

Table 6 illustrates results of data scalability. It is critical to emphasize that the tabulated results reflect foundation models pretrained with distinct data volumes, followed by **single-epoch** fine-tuning using the target city’s dataset.

### C.3 Cross-city Transfer Performance

Table 7 illustrates results of Few-shot Performance.

**Table 5: Ablation study on the SAMoE design using Acc@1**

Method	Atlanta	Chicago	Seattle	Washington	New York	Los Angeles
<b>Acc@1</b>						
w/o fuse expert	0.313	0.253	0.345	0.296	0.241	0.219
w/o moe	0.280	0.223	0.309	0.258	0.196	0.182
w/o time gate	0.316	0.256	0.348	0.298	0.243	0.223
w/o trajectory gate	0.317	0.256	0.348	0.299	0.243	0.222
w/o adapted gate	0.317	0.257	0.348	0.300	0.244	0.223
TrajMoE	0.331	0.277	0.363	0.319	0.264	0.244
<b>Acc@3</b>						
w/o fuse expert	0.456	0.359	0.498	0.440	0.372	0.327
w/o moe	0.4317	0.338	0.465	0.409	0.344	0.303
w/o time gate	0.461	0.362	0.501	0.444	0.376	0.332
w/o trajectory gate	0.462	0.362	0.502	0.445	0.375	0.330
w/o adapted gate	0.461	0.362	0.501	0.444	0.376	0.331
TrajMoE	0.467	0.371	0.509	0.452	0.386	0.341
<b>Acc@5</b>						
w/o fuse expert	0.520	0.406	0.566	0.509	0.438	0.379
w/o moe	0.505	0.393	0.542	0.486	0.420	0.363
w/o time gate	0.525	0.409	0.569	0.511	0.442	0.385
w/o trajectory gate	0.526	0.408	0.570	0.513	0.441	0.383
w/o adapted gate	0.524	0.408	0.570	0.513	0.442	0.383
TrajMoE	0.532	0.418	0.576	0.517	0.446	0.390

**Table 6: Data Scalability of pretraining**

Data volume	Atlanta	Chicago	Seattle	Washington	New York	Los Angeles
<b>Acc@1</b>						
5w	0.231	0.145	0.257	0.211	0.134	0.107
25w	0.293	0.206	0.323	0.274	0.208	0.178
50w	0.311	0.243	0.344	0.295	0.237	0.214
100w	0.331	0.277	0.363	0.319	0.264	0.244
<b>Acc@3</b>						
5w	0.364	0.219	0.392	0.336	0.229	0.182
25w	0.423	0.289	0.460	0.403	0.318	0.269
50w	0.456	0.346	0.497	0.439	0.368	0.322
100w	0.467	0.371	0.509	0.452	0.386	0.341
<b>Acc@5</b>						
5w	0.429	0.256	0.460	0.403	0.286	0.229
25w	0.485	0.328	0.525	0.468	0.377	0.317
50w	0.519	0.394	0.565	0.507	0.433	0.375
100w	0.532	0.418	0.576	0.517	0.446	0.390

**Table 7: Cross-city Transfer Performance**

Data Scale	Atlanta	Chicago	Seattle	Washington	New York	Los Angeles
<b>Acc1</b>						
1%	0.2859	0.1702	0.3129	0.2554	0.1762	0.1506
5%	0.2972	0.2151	0.3240	0.2755	0.2037	0.1771
10%	0.2989	0.2253	0.3306	0.2827	0.2123	0.1876
100%(w/o pretrain)	0.2849	0.2354	0.3210	0.2724	0.2048	0.1882
<b>Acc3</b>						
1%	0.4114	0.2473	0.4432	0.3774	0.2691	0.2359
5%	0.4290	0.2935	0.4556	0.4029	0.3079	0.2707
10%	0.4326	0.3039	0.4643	0.4108	0.3208	0.2836
100%(w/o pretrain)	0.4229	0.3395	0.4673	0.4090	0.3291	0.2890
<b>Acc5</b>						
1%	0.4726	0.2803	0.5085	0.4410	0.3192	0.2837
5%	0.4912	0.3260	0.5203	0.4679	0.3633	0.3203
10%	0.4968	0.3371	0.5299	0.4770	0.3779	0.3332
100%(w/o pretrain)	0.4875	0.3887	0.5355	0.4766	0.3941	0.3413

## References

- [1] Tom Brown, Benjamin Mann, Nick Ryder, Melanie Subbiah, Jared D Kaplan, Prafulla Dhariwal, Arvind Neelakantan, Pranav Shyam, Girish Sastry, Amanda Askell, et al. 2020. Language models are few-shot learners. *Advances in neural information processing systems* 33 (2020), 1877–1901.
- [2] Jianwei Chen, Jianbo Li, and Ying Li. 2020. Predicting human mobility via long short-term patterns. *Computer Modeling in Engineering & Sciences* 124, 3 (2020), 847–864.
- [3] Meng Chen, Yang Liu, and Xiaohui Yu. 2014. Nlpm: A next location predictor with markov modeling. In *PAKDD*. Springer, 186–197.
- [4] Riccardo Corrias, Martin Gjoreski, and Marc Langheinrich. 2023. Exploring transformer and graph convolutional networks for human mobility modeling. *Sensors* 23, 10 (2023), 4803.
- [5] Nan Du, Yanping Huang, Andrew M Dai, Simon Tong, Dmitry Lepikhin, Yanzhong Xu, Maxim Krikun, Yanqi Zhou, Adams Wei Yu, Orhan Firat, et al. 2022. Glam: Efficient scaling of language models with mixture-of-experts. In *International conference on machine learning*. PMLR, 5547–5569.
- [6] William Fedus, Barret Zoph, and Noam Shazeer. 2022. Switch transformers: Scaling to trillion parameter models with simple and efficient sparsity. *Journal of Machine Learning Research* 23, 120 (2022), 1–39.
- [7] Jie Feng, Yong Li, Chao Zhang, Funing Sun, Fanchao Meng, Ang Guo, and Depeng Jin. 2018. Deepmove: Predicting human mobility with attentional recurrent networks. In *WWW*. 1459–1468.
- [8] Sébastien Gambs, Marc-Olivier Killijian, and Miguel Núñez del Prado Cortez. 2012. Next place prediction using mobility markov chains. In *Proceedings of the first workshop on measurement, privacy, and mobility*. 1–6.
- [9] Daya Guo, Dejian Yang, Haowei Zhang, Junxiao Song, Ruoyu Zhang, Runxin Xu, Qihao Zhu, Shirog Ma, Peiyi Wang, Xiao Bi, et al. 2025. Deepseek-r1: Incentivizing reasoning capability in llms via reinforcement learning. *arXiv preprint arXiv:2501.12948* (2025).
- [10] Haoyu He, Haozheng Luo, and Qi R Wang. 2024. ST-MoE-BERT: A Spatial-Temporal Mixture-of-Experts Framework for Long-Term Cross-City Mobility Prediction. In *Proceedings of the 2nd ACM SIGSPATIAL International Workshop on Human Mobility Prediction Challenge*. 10–15.
- [11] Robert A Jacobs, Michael I Jordan, Steven J Nowlan, and Geoffrey E Hinton. 1991. Adaptive mixtures of local experts. *Neural computation* 3, 1 (1991), 79–87.
- [12] Shan Jiang, Yingxiang Yang, Siddharth Gupta, Daniele Veneziano, Shounak Athavale, and Marta C González. 2016. The TimeGeo modeling framework for urban mobility without travel surveys. *Proceedings of the National Academy of Sciences* 113, 37 (2016), E5370–E5378.
- [13] Michael I Jordan and Robert A Jacobs. 1994. Hierarchical mixtures of experts and the EM algorithm. *Neural computation* 6, 2 (1994), 181–214.
- [14] Dejiang Kong and Fei Wu. 2018. HST-LSTM: A hierarchical spatial-temporal long-short term memory network for location prediction.. In *Ijcai*, Vol. 18. 2341–2347.
- [15] Dmitry Lepikhin, Hyounjoong Lee, Yanzhong Xu, Dehao Chen, Orhan Firat, Yanping Huang, Maxim Krikun, Noam Shazeer, and Zhifeng Chen. [n. d.]. GShard: Scaling Giant Models with Conditional Computation and Automatic Sharding. In *International Conference on Learning Representations*.
- [16] Yong Li, Yuan Yuan, Jingtao Ding, and Depeng Jin. 2023. Learning the complexity of urban mobility with deep generative collaboration network. (2023).
- [17] Yan Lin, Huaiyu Wan, Shengnan Guo, and Youfang Lin. 2021. Pre-training context and time aware location embeddings from spatial-temporal trajectories for user next location prediction. In *Proceedings of the AAAI conference on artificial intelligence*, Vol. 35. 4241–4248.
- [18] Yan Lin, Tonglong Wei, Zeyu Zhou, Haomin Wen, Jilin Hu, Shengnan Guo, Youfang Lin, and Huaiyu Wan. 2024. TrajFM: A vehicle trajectory foundation model for region and task transferability. *arXiv preprint arXiv:2408.15251* (2024).
- [19] Aixin Liu, Bei Feng, Bin Wang, Bingxuan Wang, Bo Liu, Chenggang Zhao, Chengqi Deng, Chong Ruan, Damai Dai, Daya Guo, et al. 2024. Deepseek-v2: A strong, economical, and efficient mixture-of-experts language model. *arXiv preprint arXiv:2405.04434* (2024).
- [20] Qingyue Long, Can Rong, Huandong Wang, and Yong Li. 2025. One Fits All: General Mobility Trajectory Modeling via Masked Conditional Diffusion. *arXiv preprint arXiv:2501.13347* (2025).
- [21] Qingyue Long, Yuan Yuan, and Yong Li. 2024. A Universal Model for Human Mobility Prediction. *arXiv preprint arXiv:2412.15294* (2024).
- [22] Noam Shazeer, Azalia Mirhoseini, Krzysztof Maziarczyk, Andy Davis, Quoc Le, Geoffrey Hinton, and Jeff Dean. 2017. Outrageously large neural networks: The sparsely-gated mixture-of-experts layer. *arXiv preprint arXiv:1701.06538* (2017).
- [23] Junjun Si, Jin Yang, Yang Xiang, Hanqiu Wang, Li Li, Rongqing Zhang, Bo Tu, and Xiangqun Chen. 2023. Trajbert: Bert-based trajectory recovery with spatial-temporal refinement for implicit sparse trajectories. *IEEE Transactions on Mobile Computing* (2023).
- [24] Chaoming Song, Tal Koren, Pu Wang, and Albert-László Barabási. 2010. Modelling the scaling properties of human mobility. *Nature physics* 6, 10 (2010), 818–823.
- [25] Hongyuan Su, Yu Zheng, Jingtao Ding, Depeng Jin, and Yong Li. 2024. MetroGNN: Metro Network Expansion with Reinforcement Learning. In *Companion Proceedings of the ACM on Web Conference 2024*. 650–653.
- [26] Hao Sun, Changjie Yang, Liwei Deng, Fan Zhou, Feiteng Huang, and Kai Zheng. 2021. Periodicmove: Shift-aware human mobility recovery with graph neural network. In *Proceedings of the 30th ACM International Conference on Information & Knowledge Management*. 1734–1743.
- [27] Fernando Terroso-Sáenz and Andrés Muñoz. 2022. Nation-wide human mobility prediction based on graph neural networks. *Applied Intelligence* (2022), 1–17.
- [28] A Vaswani. 2017. Attention is all you need. *Advances in Neural Information Processing Systems* (2017).
- [29] Ruoxi Wang, Bin Fu, Gang Fu, and Mingliang Wang. 2017. Deep & cross network for ad click predictions. In *Proceedings of the ADKDD'17*. 1–7.
- [30] Yu Wang, Tongya Zheng, Yuxuan Liang, Shunyu Liu, and Mingli Song. 2024. Cola: Cross-city mobility transformer for human trajectory simulation. In *Proceedings of the ACM Web Conference 2024*. 3509–3520.
- [31] Song Yang, Jiamou Liu, and Kaiqi Zhao. 2022. GETNext: trajectory flow map enhanced transformer for next POI recommendation. In *Proceedings of the 45th International ACM SIGIR Conference on research and development in information retrieval*. 1144–1153.
- [32] Yuan Yuan, Jingtao Ding, Jie Feng, Depeng Jin, and Yong Li. 2024. Unist: A prompt-empowered universal model for urban spatio-temporal prediction. In *Proceedings of the 30th ACM SIGKDD Conference on Knowledge Discovery and Data Mining*. 4095–4106.
- [33] Yuan Yuan, Jingtao Ding, Chonghua Han, Depeng Jin, and Yong Li. 2024. A Foundation Model for Unified Urban Spatio-Temporal Flow Prediction. *arXiv preprint arXiv:2411.12972* (2024).
- [34] Yuan Yuan, Jingtao Ding, Chenyang Shao, Depeng Jin, and Yong Li. 2023. Spatio-temporal diffusion point processes. In *Proceedings of the 29th ACM SIGKDD Conference on Knowledge Discovery and Data Mining*. 3173–3184.
- [35] Yuan Yuan, Jingtao Ding, Huandong Wang, and Depeng Jin. 2024. Generating Daily Activities with Need Dynamics. *ACM Transactions on Intelligent Systems and Technology* 15, 2 (2024), 1–28.
- [36] Yuan Yuan, Jingtao Ding, Huandong Wang, Depeng Jin, and Yong Li. 2022. Activity trajectory generation via modeling spatiotemporal dynamics. In *Proceedings of the 28th ACM SIGKDD Conference on Knowledge Discovery and Data Mining*. 4752–4762.
- [37] Yuan Yuan, Huandong Wang, Jingtao Ding, Depeng Jin, and Yong Li. 2023. Learning to simulate daily activities via modeling dynamic human needs. In *Proceedings of the ACM Web Conference 2023*. 906–916.
- [38] Yu Zheng, Qianyu Hao, Jingwei Wang, Changzheng Gao, Jinwei Chen, Depeng Jin, and Yong Li. 2024. A Survey of Machine Learning for Urban Decision Making: Applications in Planning, Transportation, and Healthcare. *Comput. Surveys* 57, 4 (2024), 1–41.
- [39] Yu Zheng, Yuming Lin, Liang Zhao, Tinghai Wu, Depeng Jin, and Yong Li. 2023. Spatial planning of urban communities via deep reinforcement learning. *Nature Computational Science* 3, 9 (2023), 748–762.
- [40] Yu Zheng, Hongyuan Su, Jingtao Ding, Depeng Jin, and Yong Li. 2023. Road planning for slums via deep reinforcement learning. In *Proceedings of the 29th ACM SIGKDD Conference on Knowledge Discovery and Data Mining*. 5695–5706.
- [41] Yu Zheng and Xing Xie. 2011. Learning travel recommendations from user-generated GPS traces. *ACM Transactions on Intelligent Systems and Technology (TIST)* 2, 1 (2011), 1–29.
- [42] Yanqi Zhou, Tao Lei, Hanxiao Liu, Nan Du, Yanping Huang, Vincent Zhao, Andrew M Dai, Quoc V Le, James Laudon, et al. 2022. Mixture-of-experts with expert choice routing. *Advances in Neural Information Processing Systems* 35 (2022), 7103–7114.
- [43] Yuanshao Zhu, Yongchao Ye, Shiyao Zhang, Xiangyu Zhao, and James Yu. 2023. DiffTraj: Generating gps trajectory with diffusion probabilistic model. *Advances in Neural Information Processing Systems* 36 (2023), 65168–65188.
- [44] Yuanshao Zhu, James Jianqiao Yu, Xiangyu Zhao, Xuetao Wei, and Yuxuan Liang. 2024. UniTraj: Universal Human Trajectory Modeling from Billion-Scale Worldwide Traces. *arXiv preprint arXiv:2411.03859* (2024).